Properties of a class of topological phase transitions

Zi Cai,[1] Shu Chen,[1] Supeng Kou,[2] and Yupeng Wang[1]
[1]*Beijing National Laboratory for Condensed Matter Physics, Institute of Physics, Chinese Academy of Sciences, Beijing 100080, People's Republic of China*
[2]*Department of Physics, Beijing Normal University, Beijing 100875, People's Republic of China*
(Received 29 November 2007; revised manuscript received 27 March 2008; published 23 July 2008)

The properties of a class of topological quantum phase transition (TQPT) are analyzed based on a model proposed by Haldane. We study the effect of finite temperature on this phase transition. We have found that finite temperature would drive this TQPT to be a crossover, while it is stable against the weak short-range interaction. When the interaction is strong enough, however, this TQPT is unstable and other states would emerge. Then we investigate the effect of the on-site energy in the original Haldane model. The critical difference between our TQPT and the topological phase transition in conventional quantum Hall system is discussed. Finally, we discuss the potential application of our analysis to a topological phase transition proposed in a realistic system.

DOI: 10.1103/PhysRevB.78.035123 PACS number(s): 71.10.Fd, 71.30.+h, 73.43.Nq

I. INTRODUCTION

Landau's theories of the continuous phase transition have been successful and provided a paradigm in the condensed-matter physics. The spontaneous symmetry breaking plays a central role in Landau's theories. In zero temperature, however, it is possible that the change in Fermi-surface topology or the quantum fluctuation induces a new kind of phase transitions[1] beyond Landau's paradigm. The different phases in these phase transitions are not classified by different symmetries, instead, they are characterized by different topologies of Fermi surface,[2,3] different quantum numbers[4,5] or nonlocal topological order parameters,[6–8] etc. This kind of phase transition, known as topological quantum phase transition (TQPT), has attracted considerable attention in recent years because they are closely related to the field of topological quantum computation.[9] Despite great efforts, many properties of the topological phase and TQPT, such as its order and universality classes, the effect of temperature, and interaction and its stability, are still far from being completely understood. For example, since there is no spontaneous symmetry breaking in the TQPT, the Mermin–Wagner theorem[10] could not be applied to preclude the possibility of a finite-temperature phase transition in two-dimensional (2D) system. In this paper, we have partly answered the above questions.

II. HALDANE MODEL

In this paper, we present a theoretical analysis of a class of TQPT. Our starting point is the Haldane model,[11] which was proposed to study the realization of "parity anomaly" in graphenelike condensed-matter system and is another work of anomalous Hall effect (AHE). The phase transition in this model, essentially, is the transition between two phases with different parity, or in another word, different Chern numbers, which is induced by adjusting parameter to change the sign of the effective mass of the "relativistic" electrons. We show that this TQPT is a third order quantum phase transition, while most other conventional continuous quantum phase transitions are second order. We also analyze the effect of finite temperature on this TQPT; we find that there is no phase transition at $T>0$, in another words, there is no finite-temperature phase transition for the AHE. The temperature drives the TQPT to be a crossover. The critical behavior as well as the properties of correlation function in the finite temperature have also been analyzed, then an experiment is proposed to detect these unconventional properties. When there exist short-range interaction, we deal with this problem by the method of mean field and show that this TQPT is robust against the weak short-range interaction for either the repulsive or attractive case. This is very different from the regular Fermi liquid. Strong interaction would change the pictures: strong enough repulsive interaction would lead to a charge-density wave (CDW) state,[12] while strong attractive interaction would result in a superconductor.[13] To make our above results applicable to the original Haldane model, we investigate the effect of the on-site energy, which shifts the degeneracy of the two Fermi points. Furthermore, we point out the difference between this kind of TQPT and the disorder-induced localization-delocalization transition in the conventional quantum Hall systems,[14] as well as in the quantum spin Hall effect.[15,16] Finally, we show that though the Haldane model could not be realized in the present experiment, our results can be applied to a large class of TQPT which could be realized in experiment.

First, we briefly review the Haldane model[11,17] and focus on the phase transition in it. Haldane considered a $(2+1)$-dimensional $[(2+1)$-D$]$ model in which spinless fermions hop on a half-filling honeycomb lattice and couple with a periodic external magnetic field. There is no "net" magnetic flux through a unit cell and thus there is no Landau quantization. However, a next-nearest-neighbor hopping term with a phase $t_2e^{i\Phi}$ is introduced in the honeycomb lattice, which is a time-reversal breaking term and leads to a "chiral" fermions without the fermion doubling effect. This system provides a condensed-matter analog of $(2+1)$-dimensional electrodynamics[18] due to its linear energy spectrum around the Fermi point.

In the honeycomb lattice, noninteracting fermions behave as a semimetal with the Fermi-surface shrunk into two in-

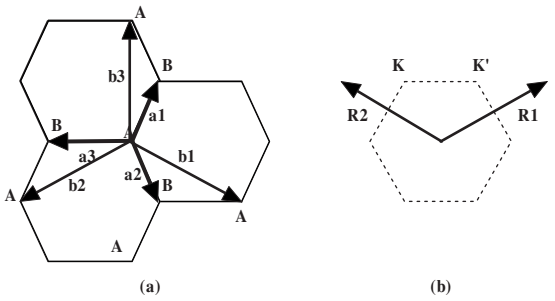

FIG. 1. (a)The honeycomb lattice as a superposition of two sublattices A and B. The basis vectors are $\mathbf{a_1},\mathbf{a_2},\mathbf{a_3}$; two sublattices are connected by $\mathbf{b_1},\mathbf{b_2},\mathbf{b_3}$. (b) The Brillouin zone, $\mathbf{R_1},\mathbf{R_2}$ are basis vector in reciprocal lattice. $\mathbf{K},\mathbf{K}'$ are two distinct Fermi point in one Brillouin zone.

equivalent points in one unit cell, as shown in Fig. 1. The general action of (2+1)-D noninteracting fermions in a uniform or periodic potential is given by

$$S = \mathrm{Tr}\int_{(2\pi)^3}^{d^3k} \Psi^\dagger(k)G^{-1}(k)\Psi(k). \tag{1}$$

For the Haldane model, it is convenient to represent G^{-1} in a basis of spinors $\Psi_k=(\Psi_{k\mathrm{A}},\Psi_{k\mathrm{B}})^T$ with A and B representing the different sublattices of the honeycomb lattice. Therefore we have

$$G^{-1} = \mathbf{I}\left[i\omega + 2t_2 \cos\Phi\sum_i \cos(\mathbf{k}\cdot\mathbf{b_i})\right] + \mathbf{d}\cdot\sigma, \tag{2}$$

where $\mathbf{d}\cdot\sigma=\Sigma_i d_i\sigma^i$, with $d_1=t_1\Sigma_i \cos(\mathbf{k}\cdot\mathbf{a_i})$, $d_2=t_1\Sigma_i \sin(\mathbf{k}\cdot\mathbf{a_i})$, $d_3=-t_2 \sin\Phi\Sigma_i \sin(\mathbf{k}\cdot\mathbf{b_i})$, and the Pauli matrices $\sigma^i(i=1,2,3)$. Here we set the on-site energy M in the original Haldane model to be zero for convenience; we would discuss the effect of M in Sec. V. t_1 and $t_2e^{i\Phi}$ are the tunneling amplitudes between the nearest- and the next-nearest neighboring sites. The parameters $\mathbf{a_1}$, $\mathbf{a_2}$, and $\mathbf{a_3}$ are the displacement from one site to its nearest neighborhoods and $\mathbf{b_1}=\mathbf{a_2}-\mathbf{a_3}$, $\mathbf{b_2}=\mathbf{a_3}-\mathbf{a_1}$, etc. We could calculate the Chern number (Hall conductance) for this model using the standard representation[19]

$$\sigma_{xy} = \frac{1}{8\pi^2}\int_\Omega d^2k[\mathbf{n}\cdot\partial_x\mathbf{n}\times\partial_y\mathbf{n}], \tag{3}$$

with $\mathbf{n}=\mathbf{d}/|\mathbf{d}|$. Finally, we could obtain

$$\sigma_{xy} = \begin{cases} 1 & \text{if } t_2\sin\Phi > 0 \\ -1 & \text{if } t_2\sin\Phi < 0 \\ 0 & \text{otherwise.} \end{cases} \tag{4}$$

The Chern number is the topological quantum number.[20] It was first introduced into the condensed-matter physics in the integer quantum Hall effect to explain the stability of the Hall conductance to weak pertubations.[21] The physical meaning of the Chern number is the quantum Hall conductance in our case. Different Chern numbers characterize different topological phases and we focus on the phase transition between them.

This phase transition could be interpreted in a traditional way by calculating the singularly of the ground-state energy. The energy spectrum for Eq. (2) is

$$E(m,\mathbf{k}) = \pm\sqrt{d_1^2+d_2^2+d_3^2}, \tag{5}$$

where d_i have been defined above and $m=t_2\sin(\Phi)$. In the ground state, the lower band is filled completely so the ground-state energy

$$E(m) = \int\int_\Omega d^2\mathbf{k} \quad E(\mathbf{k},m). \tag{6}$$

To find the singularity of $E(m)$ in the phase-transition point $m=0$, we calculate $E(m)$ and its derivative; the numerical result is shown in Fig. 2. We can see that the second derivative is continuous, while the third one is not in the phase-transition point, which means that this quantum phase transition is the third order quantum phase transition. This result could be explained in a heuristic way when we consider the behavior around the two distinct independent Fermi points. These two independent effective Hamiltonians H_α ($\alpha=1,-1$ represent different Dirac Fermi points) are given by

$$H_\alpha = \mathbf{D}_\alpha\cdot\sigma, \tag{7}$$

where $\mathbf{D}_\alpha=(\alpha k_y c, k_x c, m_\alpha)$, $c=3/2t_1$, and $m_\alpha=-3\sqrt{3}\alpha t_2 \sin\Phi$. The parameter c is the "light velocity" in the relativistic Hamiltonian and below we set $c=1$ for simplicity.

The total Hamiltonian is[11]

$$H = \Psi_{-1}^\dagger H_{-1}\Psi_{-1} + \Psi_1^\dagger H_1\Psi_1. \tag{8}$$

$\Psi_{\pm1}$ represent fermions around different Fermi points. When we adjust the parameter Φ from negative to positive, the mass of both Dirac fermions changes sign and the phase transition occurs.

Because the two Dirac Fermi points are independent with each other, below we only focus on one of them. From Hamiltonian (7), we can easily calculate the energy spectrum $E(\mathbf{k})=\pm\sqrt{\mathbf{k}^2+m^2}$, with + for the "conduction" band and − for the "valence" band. The energy of the ground state could be estimate as

$$E(m) = -\int\int d^2\mathbf{k}\sqrt{\mathbf{k}^2+m^2} = -|m|^3 + C. \tag{9}$$

C is the physical cutoff of the integral and is obviously analytic in the phase-transition point $m=0$ because we only concern about the singularity of $E(m)$ at the critical point $m=0$, C is unimportant. From Eq. (9) we find that the third order derivative of $E(m)$ to m is discontinuous in the point $m=0$, so this TQPT is a third order phase transition. The analysis above implies that Hamiltonian (8) provides an effective approximation of the actual Hamiltonian in Eq. (1) if we only concern the behavior around the Fermi point. Below we use Eq. (8) to analyze the properties of the phase transition for simplicity.

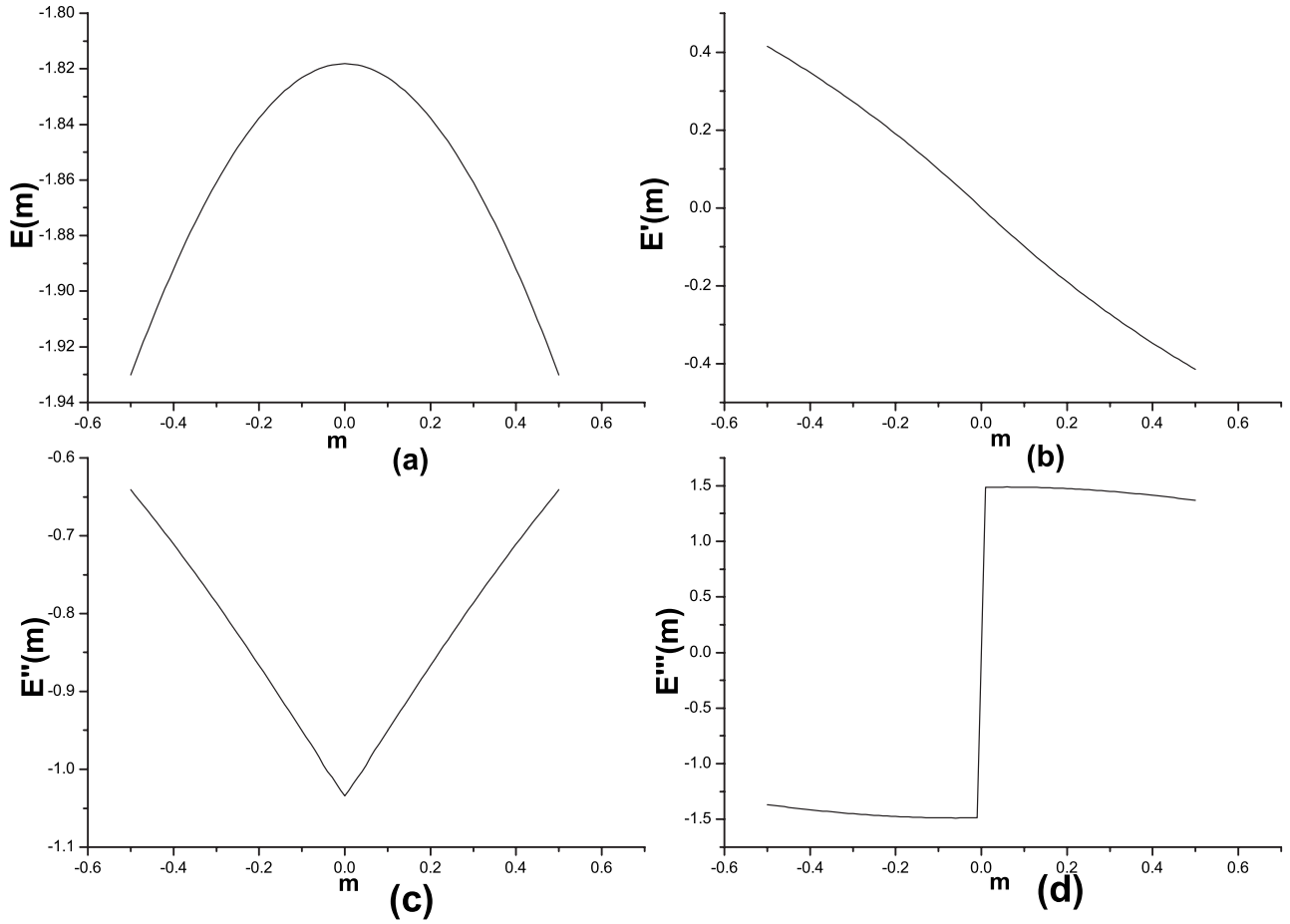

FIG. 2. (a) The ground-state energy and (b) its first-order derivative, (c) second-order derivative, and (d) third order derivative.

III. FINITE TEMPERATURE EFFECT

A typical example of finite-temperature effect on the quantum phase transition is the transverse Ising model,[1] which is fermionized by the Jordon–Wigner transformation. The finite temperature drives the quantum phase transition into a crossover. It is shown that there is a similar behavior in our case. When the temperature is not too high, the model could be expressed in terms of a continuum canonical fermion field $\Psi=(\Psi_\uparrow,\Psi_\downarrow)^T$. Its partition function is

$$Z_F=\int D\Psi^\dagger(\mathbf{x},\tau)D\Psi(\mathbf{x},\tau)\exp\left(-\int_0^{1/T}d\tau\int d^2\mathbf{x}L_F\right), \tag{10}$$

with

$$L_F=\Psi_{-1}^\dagger\left(\frac{\partial}{\partial\tau}+\partial_x\sigma^y+\partial_y\sigma^x-m\sigma^z\right)\Psi_{-1}+\Psi_1^\dagger\left(\frac{\partial}{\partial\tau}+\partial_x\sigma^y-\partial_y\sigma^x+m\sigma^z\right)\Psi_1. \tag{11}$$

Here τ is the imaginary time. From Eqs. (10) and (11), we perform the standard scaling transformation by rescaling lengths, times, as well as the field. We define $x'=xe^{-l}$, $\tau'=\tau e^{-zl}$, $\Psi'=\Psi e^l$, with e^{-l} being the dimensional rescaling factor. To make sure the new L_F having the same form in terms of x',τ',Ψ', we find that $z=1$ and $m'=me^l$. So we have $\dim[m]=1$ and the critical exponent $\nu=1$.

At finite temperature T, the free energy F is given by

$$F=-T\int\frac{d^2\mathbf{k}}{(2\pi)^2}2\ln[\cosh(\sqrt{\mathbf{k}^2+m^2}/T)]. \tag{12}$$

To find out whether there is a finite-temperature phase transition, we should calculate the derivative of the free energy. Numerical results are shown in Fig. 3. [Because we only consider the singularities around the phase-transition point, we set a physical cutoff of the integral and it would not effect the singularities of Eq. (12).] We can see that the free energy is analytic; there is no singularity in Eq. (12) at $T\neq 0$, thus no phase transition occurs. However, there is a crossover just like in the transverse Ising model at finite temperature. The phase diagram is shown in Fig. 2. There are two regions in the phase diagram: the low-T massive Chiral liquid and the continuum high-T region (quantum-critical region). However, the temperature could not be too high that the continuum action L_F in Eq. (11) fails to provide a good approximation of the real system. Below we analyze the properties in both regions by calculating the fermion Green's function: $G_F(\mathbf{x},t)=\langle\Psi(\mathbf{x},t)\bar{\Psi}(0,0)\rangle$. In the quantum-field theory, the

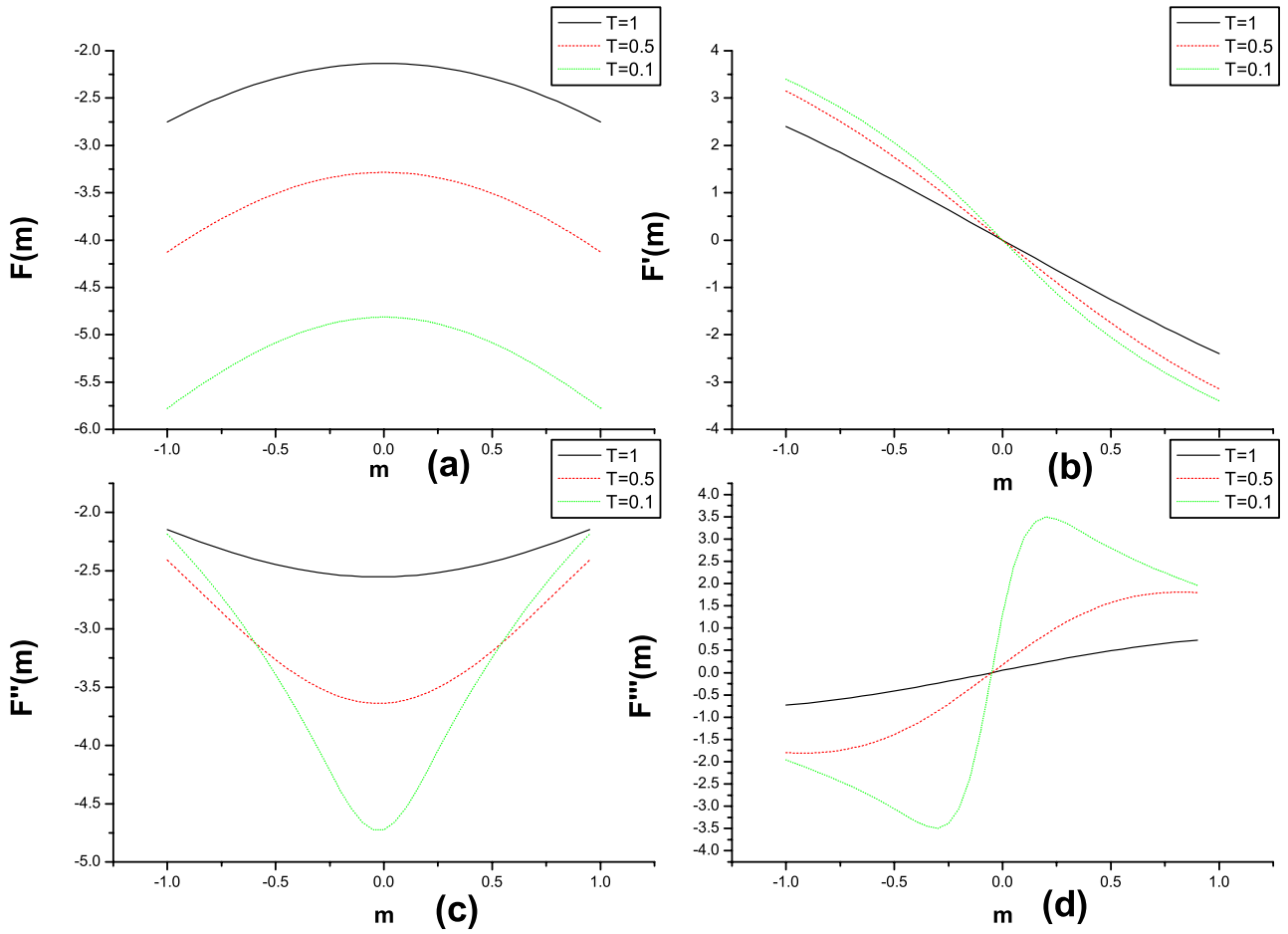

FIG. 3. (Color online) (a) The free energy and (b) its first-order derivative, (c) second-order derivative, and (d) third order derivative at different temperatures.

Green's function for the massive Dirac fermions at finite temperature is

$$G_F^{ab}(\mathbf{x},t) = (i\gamma^\mu \partial_\mu + m)_{ab} g_F(\mathbf{x},t), \tag{13}$$

$$g_F(\mathbf{x},t) = -\int \frac{d^2\mathbf{k}}{(2\pi)^2} \frac{1}{\sqrt{\mathbf{k}^2+m^2}} \frac{e^{-i\mathbf{k}\cdot x + i\sqrt{\mathbf{k}^2+m^2}t}}{1+e^{\sqrt{\mathbf{k}^2+m^2}/T}}. \tag{14}$$

We use the 2D representation of γ matrix ($\mu=0,1,2$) rather than the ordinary four-dimensional (4D) representation. a,b is the spin of the Dirac electron. t denotes the real time, as shown in Fig. 4.

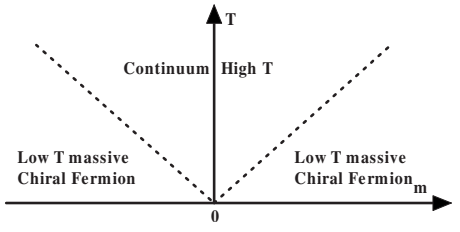

FIG. 4. Finite-T phase diagram of the TQPT as a function of the mass **m** of the Dirac fermion and the temperature T.

In our case, there are two kinds of Dirac fermions (Ψ_1 and Ψ_{-1}) and both of them contribute to the Green's function, the Green function is slightly different from standard formula (13), as we will show below.

A. *Low-T massive Dirac liquid*, $T \ll |m|$

In this region, the temperature is very low and thus the physics is controlled primarily by the critical line $T=0$. First we analyze $T=0$ equal-time correlations given by

$$g_F(\mathbf{x},0) = -\int \frac{d^2\mathbf{k}}{(2\pi)^2} \frac{e^{-i\mathbf{k}\cdot x}}{\sqrt{\mathbf{k}^2+m^2}} = \int_0^\infty \frac{dk}{2\pi} \frac{kJ_0(k|x|)}{\sqrt{k^2+m^2}}. \tag{15}$$

We could approximately estimate the asymptotic behavior when $|\mathbf{x}| \to \infty$ by the contour integration which picks up contribution from the poles at which function is divergent in the complex k plane. For large x, those poles closest to the real axis provide the dominant contribution to the integral. The leading result is $G(|\mathbf{x}|,0) \approx C(x)e^{-|m||\mathbf{x}|}$ ($|\mathbf{x}| \to \infty$), and thus the equal-time correlation exponentially decays in the spatial dimension with a correlation length $\xi = 1/|m|$.

Then we calculate the equal-space correlation. For $T=0$, we have

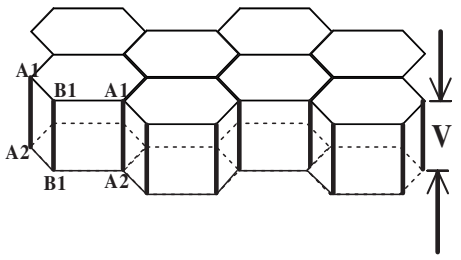

FIG. 5. The bilayer Haldane model with voltage V between the layers. The I-V curve of the tunneling current could be measured in this device.

$$g(0,t) = -\int \frac{d^2\mathbf{k}}{(2\pi)^2} \frac{e^{i\sqrt{\mathbf{k}^2+m^2}t}}{\sqrt{\mathbf{k}^2+m^2}}. \tag{16}$$

Doing this integration directly, we get

$$g(0,t) \propto \frac{1}{it} e^{i|m|t}. \tag{17}$$

So we find

$$G^{AA}(0,t) \propto -\frac{1}{it^2} e^{i|m|t} + \frac{|m|}{t} e^{i|m|t}. \tag{18}$$

We notice that the term m in Eq. (13) does not appear in Eq. (18) because the m in different Fermi points have opposite sign and cancel each other so $G(0,t)$ is independent of the sign of m, which is reasonable in physics.

So $G(0,t)$ decays with a power law and oscillatory with a frequency $|m|$. The correlation length in the real time axis (coherent time) is infinite when $T=0$. We can see that though there is a gap, quantum systems at $T=0$ indeed have a long-range phase correlation in time which could not be seen when we map the D-dimensional quantum system to the $(D+1)$-dimensional classic system.[1] When the temperature is very low, the density of the quasiparticles is small, so the life of a quasiparticle (coherent time) holds for a long time in this region.

Now we discuss the observable effect of $G(0,t)$ in this region. We use the tunneling effect in a bilayer Haldane model. There is a voltage V between the bilayer. By calculating the I-V curve in the our system, we can find that it is totally different from the ordinary electron systems, as shown in Fig. 5.[6]

Notice that we only consider the long-term behavior of $G(0,t)$ in experiment, which is $t \gg \frac{1}{|m|}$ (actually it is $t \gg \frac{\hbar}{|m|}$, we set $\hbar=1$ in our case). So $|m|/t \gg 1/t^2$, the term $\frac{1}{it^2} e^{i|m|t}$ is neglectable in Eq. (18), so $G^{AA}(0,t) \propto \frac{|m|}{t} e^{i|m|t}$. The correlation of the tunneling operator $I(t)=C_{1A}^{\dagger}(0,t)C_{2A}(0,t)$ is

$$\langle I(t)I^{\dagger}(0)\rangle = -G_1^{AA}(t,0)G_2^{AA}(-t,0) \propto \frac{m^2}{t^2},$$

where 1, 2 denote the different layers and A, B are different sublattices in each layer. Using the linear-response formation, it is easy to find that the tunneling current $I \propto m^2 V$, which is different from the massless case $I \propto V^3$.

B. *Continuum high-T region*, $T \gg |m|$

This region is also known as the "quantum-critical region," which plays an important role in condensed-matter physics because of its potential relation with the heavy fermion systems[22] and the high-T_C superconductivity.[23] The de Broglie wavelength of the excitation in this region is the same order as their mean spacing, so quantum and thermal effects entangle and both of them play an equally important role.[24] We mainly focus on the line $m=0$ and calculate the equal-space correlation to see how the effect of temperature changes the behavior [Eq. (13)]. Hence

$$g(0,t) = -\int \frac{d^2\mathbf{k}}{(2\pi)^2} \frac{e^{i|k|t}}{|k|(1+e^{-|k|/T})} = \int_0^{\infty} \frac{dk}{2\pi^2} \frac{e^{ikt}}{1+e^{-k/T}}. \tag{19}$$

This integral could be done by the contour integration. In the experimental condition, $t \gg \hbar/k_B T$ (we set $k_B=\hbar=1$ in our case), it is easy to find that

$$G(0,t) \propto T^2 e^{-\pi t T}. \tag{20}$$

We can see that Eq. (21) is totally different from Eq. (18). The equal-space correlation decays exponentially and the phase-coherent time is proportional to $1/T$ in this region.

IV. SHORT-RANGE INTERACTION

For fermions, the interaction and interaction-induced quantum phase transition play a central role in condensed-matter physics.[25,26] We will show that our TQPT is stable against both the weak repulsive and attractive interaction, while strong enough repulsive/attractive interaction would lead to the CDW/superconductor state.

First we consider the condition in the critical point of the TQPT ($m=0$). The Hamiltonian for the spinless fermions in the honeycomb lattice with nearest-neighbor interaction V is given by

$$H = \sum_i \sum_{\mathbf{a}} \left[-\frac{1}{2}(a_i^{\dagger} b_{i+\mathbf{a}} + \text{H.c.}) + V\left(n_i^a - \frac{1}{2}\right)\left(n_{i+\mathbf{a}}^b - \frac{1}{2}\right)\right], \tag{21}$$

where $\mathbf{a}$ is the displacement from one site to its nearest-neighbor site. For the repulsive interaction, we use the standard mean field to deal with the interaction. Assuming $\langle n_i \rangle = 1/2 + 1/2(-1)^i \Delta$, with $i=0$ for $i \in A$ and $i=1$ for $i \in B$, we get

$$H = \sum_i \sum_{\mathbf{a}} \left[-\frac{1}{2}(a_i^{\dagger} b_{i+\mathbf{a}} + \text{H.c.}) + V\left(\frac{\Delta^2}{4} - \Delta(-1)^i n_i\right)\right]. \tag{22}$$

Following the standard procedure,[26] we calculate the energy of the ground state. Minimize it with respect to Δ, we obtain the self-consistent equation,

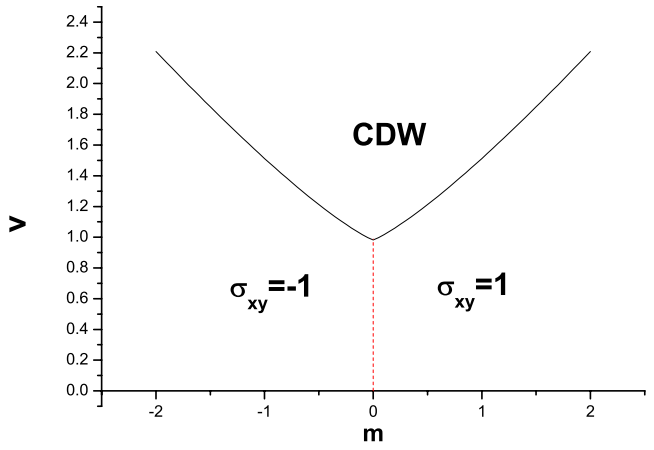

FIG. 6. (Color online) The phase diagram of the TQPT with the next-nearest interaction **V**; the solid line is the phase boundary between the CDW and topological phases and the dot line is the phase boundary of our TQPT.

$$1 = V\int \frac{d^2\mathbf{k}}{(2\pi)^2}\frac{1}{\sqrt{E^2(\mathbf{k})+\Delta^2 V^2}}, \tag{23}$$

with $E^2(\mathbf{k})=4\cos^2(k_x/2)+4\cos(\sqrt{3}k_y/2k_y)\cos(k_x/2)+1$ at the critical point $(m=0)$. When we deviate from the critical point, there is a mass term in $E^2(\mathbf{k})$, and it is estimated that $E^2(\mathbf{k},m)\approx 4\cos^2(k_x/2)+4\cos(\sqrt{3}k_y/2)\cos(k_x/2)+1+m^2$.

By solving this equation, we find that there is a SM-CDW transition at a finite value $V_c(m)=0.98$. The numerical result is shown in Fig. 6. For the weak interaction $V<V_c$, $\Delta=0$, and the TQPT is stable. It is consistent with previous study of the chiral symmetry breaking induced by Coulomb interaction in layered graphite.[27] For attractive interaction, a mean field similar to the BCS theory could be done. The SM-superconductor phase transition in the honeycomb lattice has been analyzed.[13,28] These works support the result that, for the half-filling fermions, there exists a SM-superconductor phase transition in $V=-V_c$ and when $V>-V_c$, the SM is stable. This result is also correct when m deviates from 0 slightly, so our TQPT is stable for the weak attractive interaction.

In addition, it is interesting to study the effect of the temperature in the global phase diagram in Fig. 6: In the CDW phase, it is known that there is a finite-temperature phase transition for the 2D CDW system. When the temperature is high enough, the CDW order is destroyed. However, for the topological phase, as analyzed above, there is no thermodynamic phase transition at finite temperature; this result has shown a critical difference between the topological phase and nontopological phase.

V. EFFECT OF THE ON-SITE ENERGY *M*

Up to now, we assume the on-site energy in the original Haldane model $M=0$. As a consequence, the two kinds of Dirac fermions ψ_1 and Ψ_{-1} degenerate and the effective mass of them $m_\alpha=-3\sqrt{3}\alpha t_2 \sin\Phi$. At the phase transition point, the mass of both kinds of fermions changes sign simultaneously; thus the Chern number of the whole system changes from −1 to +1. When the on-site energy M is included, as in the original Haldane model, the condition is different. Now the effective mass of the two kinds of Dirac fermions $m_\alpha=M-3\sqrt{3}\alpha t_2 \sin\Phi$, thus the energy of them no longer degenerate. The phase diagram with M has been demonstrated by Haldane (Fig. 7). We assume $M>0$, as shown in Fig. 7, when the original critical point $\Phi=0$ is split into two different phase-transition points, $\Phi_\alpha=\alpha\sin^{-1}(M/3\sqrt{3}t_2)$ and $\alpha=\pm 1$. At the point of Φ_+, for instance, only the mass of one kind of Ψ_{-1} changes sign, while the other is not, thus the Chern number of the whole system is changed from +1 to 0, different from the condition when we set $M=0$. At this phase-transition point, we will find that only one kind of Dirac fermions experiences the same singularity, as shown in Fig. 2, while the energy of the other one is analytic in this transition point. However, if we only focus on the properties of the phase-transition point, the analytic part is not important, so all the results in Secs. I and IV can be applied to this kind of phase transition, which is a third order quantum phase transition. The temperature would drive it to be a crossover and the weak interaction cannot change the TQPT.

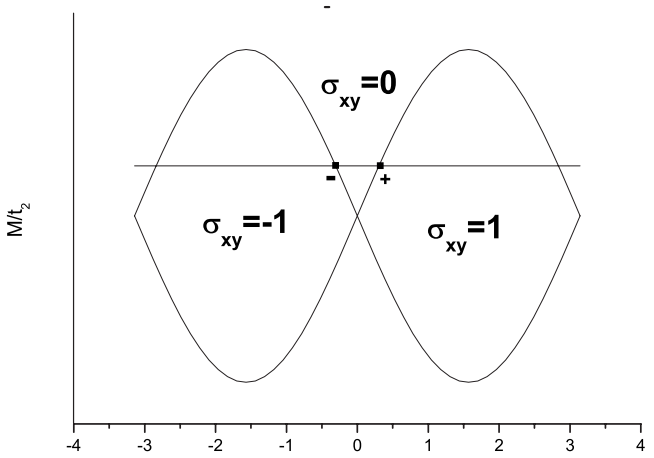

FIG. 7. The phase diagram in the original Haldane model. The on-site energy M shifts the degeneracy between the two Fermi points and splits our original TQPT into two TQPTs $(+,-)$.

VI. APPLICATION AND DISCUSSION

Now we discuss the important difference between our TQPT and one of the most typical TQPTs, i.e., the disorder-induced localization-delocalization transition between different Hall plateaus in the quantum Hall effect.[14,29] This kind of phase transition is controlled by the impurity and it is, in nature, a kind of percolation phase transition with a critical exponent $\nu=7/3$. In our TQPT, however, there are no impurities and the phase transition is controlled by the mass of Dirac fermions. From the analysis above, we can get that $\nu=1$. So our TQPT is totally different from the phase transition in Ref. 14. It is also different from the localization-delocalization transitions in the quantum spin Hall effect[15] with $\nu=1.66$.

Since the Haldane model is an artificial model which could not be realized easily in experiments, we would turn to

other physical systems in order to find this TQPT experimentally. In a recent work about quantum spin Hall effect,[5,30] an experiment in HgTe quantum well is proposed to realize this TQPT. This simplified model is based on the $\mathbf{k}\cdot p$ perturbation theory. For each kind of electrons with spin $\uparrow$ or $\downarrow$, there is a Dirac-type subband due to the special structure of the quantum well. When the thickness of quantum well is adjusted to a certain point, the effective mass of two kinds of Dirac electrons would change its sign and a TQPT occurs. The system does not break the time-reversal invariance, thus there is no Hall conductance, instead, there exists a quantum jump of the spin Hall conductance $\Delta\sigma_{xy}^{s}=\frac{2e^2}{h}$. However, there is a difference between this TQPT and our case. The mass term in Ref. 5 is $\mathbf{k}$ dependent: $m=m^{*}-ck^2$, which makes their Hamiltonian different from the standard Dirac fermion. This difference results that the phase transition is no longer between two symmetric phase with the topological number $\sigma=\pm 1$ but between a spin Hall insulator ($\sigma^{s}=0$) and a spin Hall conductance ($\sigma^{s}=2$). However, if we only focus on the phase transition, simple scaling analysis implies that the term k^2 is relevant in the phase-transition point, so our results in this paper could be applied to this TQPT.

It is natural to ask what happens if the interaction is long range (Coulomb interaction), which corresponds to the more physical situation. Since the weak short-range interaction is irrelevant in the critical point ($m=0$), simple scale analysis would imply that the TQPT is still stable for the weak long-range interaction. However, when the interaction is strong enough, the situation is complex and whether there is a phase transition driven by the interaction is still controversial.[31] To answer this question, it is necessary to do the renormalization-group analysis of the $(2+1)$-dimensional massive QED coupling with the gauge field.

Note added in proof. After our paper was accepted for publication, we were informed that similar thermal effects on the free energy of the Kitaev's and Wen's models was discussed in Ref. 32.

[1] S. Sachdev, *Quantum Phase Transitions* (Cambridge University Press, Cambridge, 1999).
[2] I. M. Lifshiz, Sov. Phys. JETP **11**, 1130 (1960).
[3] G. E. Volovik, *The Universe in a Helium Droplet* (Clarendon, Oxford, 2003).
[4] N. Read and D. Green, Phys. Rev. B **61**, 10267 (2000).
[5] B. A. Bernevig, T. L. Huge and S. C. Zhang, Science **314**, 1757 (2006).
[6] X. G. Wen, *Quantum Field Theory of Many-Body Systems* (Oxford University Press, Oxford, 2004).
[7] X. Y. Feng, G. M. Zhang, and T. Xiang, Phys. Rev. Lett. **98**, 087204 (2007).
[8] J. Yu, S. P. Kou, and X. G. Wen, arXiv:quant-ph/0709227 (unpublished).
[9] S. Das Sarma, M. Freedman, and C. Nayak, Phys. Today **59**(7), 32 (2006).
[10] N. D. Mermin and H. Wagner, Phys. Rev. Lett. **17**, 1133 (1966).
[11] F. D. M. Haldane, Phys. Rev. Lett. **61**, 2015 (1988).
[12] I. F. Herbut, Phys. Rev. Lett. **97**, 146401 (2006).
[13] B. Uchoa and A. H. Castro Neto, Phys. Rev. Lett. **98**, 146801 (2007).
[14] B. Huckestein, Rev. Mod. Phys. **67**, 357 (1995).
[15] M. Onoda, Y. Avishai, and N. Nagaosa, Phys. Rev. Lett. **98**, 076802 (2007).
[16] T. Senthil, J. B. Marston, and M. P. A. Fisher, Phys. Rev. B **60**, 4245 (1999).
[17] V. M. Yakovenko, Phys. Rev. Lett. **65**, 251 (1990).
[18] G. W. Semenoff, Phys. Rev. Lett. **53**, 2449 (1984).
[19] X. L. Qi, Y. S. Wu, and S. C. Zhang, Phys. Rev. B **74**, 085308 (2006).
[20] D. J. Thouless, *Topological Quantum Numbers in Nonrelativistic Physics* (World Scientific, Singapore, 1998).
[21] Q. Niu, D. J. Thouless, and Y. S. Wu, Phys. Rev. B **31**, 3372 (1985).
[22] F. Steglich, B. Buschinger, P. Gegenwart, M. Lohman, R. Helfrich, C. Langhammer, P. Hellman, L. Donnevert, S. Thomas, A. Link, C. Geibel, M. Lang, G. Sparn, and W. Assmus, J. Phys.: Condens. Matter **8**, 9909 (1996).
[23] C. M. Varma, Phys. Rev. Lett. **83**, 3538 (1999).
[24] S. Das Sarma, E. H. Hwang, and W.-K. Tse, Phys. Rev. B **75**, 121406(R) (2007).
[25] J. A. Hertz, Phys. Rev. B **14**, 1165 (1976).
[26] R. Shankar, Rev. Mod. Phys. **66**, 129 (1994).
[27] D. V. Khveshchenko, Phys. Rev. Lett. **87**, 246802 (2001).
[28] E. Zhao and A. Paramekanti, Phys. Rev. Lett. **97**, 230404 (2006).
[29] S. L. Sondhi, S. M. Girvin, J. P. Carini, and D. Shahar, Rev. Mod. Phys. **69**, 315 (1997).
[30] X. Dai, T. L. Hughes, X. L. Qi, Z. Fang, and S. C. Zhang, Phys. Rev. B **77**, 125319 (2008).
[31] D. T. Son, Phys. Rev. B **75**, 235423 (2007).
[32] Z. Nussinov and G. Ortiz, arXiv:cond-mat/0702377v5 (unpublished).